Magnetic and Electrical Separation, Vol. 11(3), pp. 169–188

Taylor & Francis
Taylor & Francis Group

FEATURES OF MOTION OF PARAMAGNETIC PARTICLES NEAR THE EQUILIBRIUM POINTS OF THE WORK ZONE OF A MAGNETIC SEPARATOR

YU. S. MOSTYKA*, V.I. KARMAZIN,
V. YU. SHUTOV and L.Z. GREBENYUK

National Mining University of the Ukraine, 19, Karl Marks prospect, 49027, Dnepropetrovsk, The Ukraine

(Received 3 September 2001; In final form 30 December 2001)

The oscillation of paramagnetic particles near the equilibrium point in the working gap of a magnetic separator with cylindrical elements was considered. Using the results of numeric calculation of a paramagnetic particle motion equation, the dependencies of particle oscillation amplitude on main parameters (diameter and density of particle, diameter of cylinder, carrying fluid velocity and viscosity, magnetic field strength and magnetic susceptibility of particle) were investigated. For a various combination of the parameters the relative time of particle motion was also calculated as a dependence upon the trajectory displacement compared to limiting trajectory.

Keywords: Magnetic separation; Particle trajectory; Oscillation of paramagnetic particle

1. INTRODUCTION

The efficiency of magnetic separation varies depending on several technological parameters and also on a great number of physical properties of weakly magnetic particles. To define an optimal combination of all these characteristics is an intractable problem. One of the ways to solve it is to analyze some features of motion of the particles near

*Corresponding author.

ISSN 1055-6915 print: ISSN 1477-2876 online © 2002 Taylor & Francis Ltd
DOI: 10.1080/10556910290009021

a ferromagnetic collector: these features may have a substantial influence upon the formation of the particle build-up. Some of such features are an oscillation character of motion of paramagnetic particles near equilibrium points in some regimes, the decrease of the velocity of motion of the particles and a probable increase of their concentration near the points of equilibrium, crossing of the particle trajectories etc.

2. A THEORETICAL MODEL

Works [1,2] and some others show that in a work zone of a magnetic separator with ferromagnetic collectors, trajectories of magnetic particles may have a point of equilibrium; in this point the particle velocity relative to the collector may be almost equal to zero and the direction of motion changes abruptly. More detailed calculations show that under some conditions the particle motion near the equilibrium point has an oscillating character. In this work we consider the influence of the most important parameters (particle size, their density, magnetic susceptibility, flow velocity and viscosity of the liquid, magnetic field strength, diameter of cylindrical ferromagnetic elements etc.) on the amplitude of oscillation of the particles, when the particle trajectory is limiting. A term "limiting trajectory" has been used before in [1] and means a trajectory, which divides a set of captured particles trajectory and a set of non-captured one.

Let's use differential equations of motion of magnetic particles near a ferromagnetic collector as presented in [3]:

$$\frac{d^2r}{dt^2} - r\left(\frac{d\theta}{dt}\right)^2 = \frac{1}{Q_p}\left[-\frac{\upsilon_m}{\tilde{r}^3}\left(\frac{A}{\tilde{r}^2} + \cos 2\theta\right) - N_d(\upsilon_{p,r} - \upsilon_{f,r})\right] + g\left(1 - \frac{\rho_f}{\rho_p}\right)\cos(\theta - \beta); \tag{1}$$

$$r\frac{d^2\theta}{dt^2} + 2\frac{dr}{dt}\frac{d\theta}{dt} = \frac{1}{Q_p}\left[-\frac{\upsilon_m}{\tilde{r}^3}\sin 2\theta - N_d(\upsilon_{p,\theta} - \upsilon_{f,\theta})\right] - g\left(1 - \frac{\rho_f}{\rho_p}\right)\sin(\theta - \beta), \tag{2}$$

where t is the time; r, θ are the radial and azimuthal coordinates of the polar system, the center of which coincides with the center of the cross section of cylindrical elements of the matrix;

$$\upsilon_m = \mu_0(\kappa_p - \kappa_f)\frac{d_p^2}{18\eta}\frac{MH_0}{r_w} \quad \text{or} \quad \upsilon_m = (\kappa_p - \kappa_f)\frac{d_p^2}{18\eta}\frac{MB_0}{r_w}; \quad Q_p = \frac{\rho_p d_p^2}{18\eta}$$

d_p is the particle diameter;

$$\tilde{r} = \frac{r}{r_w}$$

r_w is the radius of the cylindrical element; κ_p, κ_f are volumetric magnetic susceptibilities of the particles and of carrying fluid, respectively, η is the dynamic viscosity of the carrying fluid; H_0 and B_0 are the external magnetic field strength and induction respectively; $M = 2AH_0$ is the collector magnetization (under the condition of saturation $M = M_s$, where M_s is the saturation magnetization);

$$A = \frac{\mu_w - \mu_f}{\mu_w + \mu_f}$$

μ_w, μ_f are the magnetic permeabilities of collector and carrying fluid respectively, ($\mu_f \approx \mu_0$); $\upsilon_{p,r}$ and $\upsilon_{f,r}$ are the radial components of the vectors $\vec{\upsilon}_p$ and $\vec{\upsilon}_f$ of the particle and fluid velocities; $\upsilon_{p,\theta}$ and $\upsilon_{f,\theta}$ are the azimuthal components of vectors $\vec{\upsilon}_p$ and $\vec{\upsilon}_f$; ρ_p, ρ_f are the particle and fluid densities;

$$N_d = C_d/C_{d,0}$$

$C_{d,0}$ and C_d are hydrodynamic drag coefficients determined from the Stokes formula and from a more general formula for arbitrary Reynolds form number; g is the acceleration of gravity; β is the angle between x axis and vector $\vec{g}$.

The functions $\upsilon_{f,r}(r, \theta)$ and $\upsilon_{f,\theta}(r, \theta)$ which are used in Eqs. (1) and (2) correspond to the potential flow around a cylinder.

Equations (1) and (2) may have points of equilibrium (bifurcation points) under some conditions. Let us consider some assumptions,

which allow us to simplify the equations of particle motion and in this way to obtain an analytical solution of equilibrium point coordinates:

1. The hydrodynamic drag force of a particle is determined by the Stokes formula;
2. The gravitational force is considered to be zero;
3. Components of the carrying medium velocity are determined by the formula for the potential flow around a cylinder, when the velocity vector of the unperturbed flow $\vec{v}_0$ is normal to the axis of the cylinder.

Considering these assumptions for the so-called longitudinal configuration [1], when the vector of velocity $\vec{v}_0$ is parallel to the vector of magnetic induction $\vec{B}_0$, we can determine coordinates of the equilibrium point from the system of equations:

$$\frac{v_m}{v_0}\frac{1}{\tilde{r}^3}\left(\frac{A}{\tilde{r}^2}+\cos 2\theta\right)+\left(1-\frac{1}{\tilde{r}^2}\right)\cos\theta=0; \tag{1a}$$

$$\frac{v_m}{v_0}\frac{\sin 2\theta}{\tilde{r}^3}-\left(1+\frac{1}{\tilde{r}^2}\right)\sin\theta=0. \tag{2a}$$

We can also obtain an analogous equation for the case of the so-called transversal configuration, when $\vec{v}_0 \perp \vec{B}_0$.

From the system of Eqs. (1a) and (2a) we can deduce, by making some transforming, the equation for the radial coordinate r:

$$\tilde{r}^8+\tilde{r}^6-\tilde{r}^2\left(\frac{v_m}{v_0}\right)^2+A\left(\frac{v_m}{v_0}\right)^2=0 \tag{3}$$

or

$$x^4+x^3-x\omega+A\omega=0, \tag{3a}$$

where

$$x=\tilde{r}^2; \quad \omega=\left(\frac{v_m}{v_0}\right)^2 \tag{4}$$

When $A=0$, we can reduce the equation of fourth order (3a) to the cubic equation (taking into account that $x \neq 0$, since $r \neq 0$):

$$x^3 + x^2 - \left(\frac{\upsilon_m}{\upsilon_0}\right)^2 = 0. \tag{5}$$

Madai [2] found analytical solution for this case.

Let's emphasize that such a solution (in the form of cubic equation for the unknown $x = \tilde{r}^2$) is possible in the case of three assumptions mentioned above and with additional restriction $A=0$. The last assumption is approximately correct under the condition of very high values of the magnetic field strength H_0. If the real case $A > 0$ is considered (and, as before, the three aforesaid assumptions are accepted), the radial coordinate of the equilibrium point may be determined by solving Eq. (3a) for unknown x and the following substitution, taking into account Eq. (4): $\tilde{r} = \sqrt{x}$. Then we insert the received value $\tilde{r}$ in the Eq. (2a) and then find the azimuthal coordinate θ of the equilibrium point from it.

The equation of the fourth order (3a) has four roots, which may be found as solutions of two quadratic equations:

$$x^2 + \frac{1}{2}(1 + R_{1,2})x + y + \frac{y+\omega}{R_{1,2}} = 0, \tag{6}$$

where

$$R_1 = \sqrt{8y+1}; \tag{7a}$$

$$R_2 = -\sqrt{8y+1}, \tag{7b}$$

y is a real root of the cubic equation:

$$y^3 - \omega\left(\frac{1}{4} + A\right)y - \frac{\omega}{8}(A+\omega) = 0. \tag{8}$$

Solution of the last equation for y can be written as:

$$
\begin{aligned}
y &= \sqrt[3]{-\frac{q}{2}+\sqrt{Q}}+\sqrt[3]{-\frac{q}{2}-\sqrt{Q}}, \\
Q &= \frac{q^2}{4}+\frac{p^3}{27}; \\
p &= -\omega\left(\frac{1}{4}+A\right); \\
q &= -\frac{\omega}{8}(A+\omega); \\
\omega &= \left(\frac{v_m}{v_0}\right)^2.
\end{aligned}
\tag{9}
$$

The case of $Q > 0$ is considered.

Using the found value y in Eqs. (7a), (7b) and (6), we can find four roots for $x(x = \tilde{r}^2)$:

$$
\begin{aligned}
x_{1,2} &= -\frac{p_*}{2} \pm \sqrt{\frac{p_*^2}{4}-q_*}; \\
p_* &= \frac{1}{2}(1+R_{1,2}); \\
q_* &= y+\frac{y+\omega}{R_{1,2}}.
\end{aligned}
$$

Then we find four roots for the radial coordinate of the equilibrium point

$$
\begin{aligned}
(\tilde{r}_*)_{1,2} &= \sqrt{x_1(R_{1,2})}; \\
(\tilde{r}_*)_{3,4} &= \sqrt{x_2(R_{1,2})}.
\end{aligned}
$$

Finally, we choose the roots according to the physical sense of the problem.

It is evident that the analytical solution for the coordinate of the equilibrium point in the case of $A > 0$ (the case of $A = 0$ has been considered by Madai) becomes rather complicated and bulky, even if we assume that the hydrodynamic drag on the particle is determined by the Stokes formula and that we can disregard the gravitational force. Taking into account that conditions of flow around the particle

in a general case differ from Stokes regime, it's impossible to obtain analytical solution. In this case, and also taking into account gravitational force we use more complicated equations, which can be solved by numerical methods, instead of the system of Eqs. (1a) and (2a), to determine the coordinates of the equilibrium point.

3. DISCUSSION OF RESULTS

Let us consider some results of calculations of the amplitude of particle oscillation near the equilibrium point, time of a particle motion depending on the trajectory proximity to the limit trajectory, and also the change of particle concentration near the equilibrium point. The particle trajectories were calculated by solving numerically system of differential Eqs. (1) and (2).

3.1 The Influence of Particle Properties and Characteristics of Separation Process on the Amplitude of Particle Oscillations

Let us consider the following factors influencing the oscillation amplitude: particle diameter d_p, diameter of cylindrical ferromagnetic element d_w, unperturbed flow velocity $_0$, external magnetic induction B_0, specific magnetic susceptibility of particle χ_p, density of particle ρ_p. The calculations have been carried out ignoring the gravitational force F_g and taking into account different orientations of vector $\vec{F}_g$ relatively to vectors $\vec{\upsilon}_0$ and $\vec{B}_0$.

The results of calculations of the limiting trajectories of a particle with diameter $d_p = 200\,\mu\text{m}$, when the cylinder diameter is $d_w = 1\,\text{mm}$ and the flow velocity is $\upsilon_0 = 0,1\,\text{m/s}$ for ilmenite particles (density $\rho_\text{p} = 4.7 \times 10^3\,\text{kg/m}^3$ and magnetic susceptibility $\chi_\text{p} = 1.5 \times 10^{-6}\,\text{m}^3/\text{kg}$, curves 1 and 2) and wolframite particles (density $7.5 \times 10^3\,\text{kg/m}^3$ and magnetic susceptibility $0.6 \times 10^{-6}\,\text{m}^3/\text{kg}$, curve 3,4,5) are shown in the Fig. 1. Curve 1 was calculated for $B_0 = 0.25$ T, curves 2 to 5: $B_0 = 0.5$ T; curves 1–3, 5: $g = 0$; curve 4: $g = 9.81\,\text{m/s}^2$; $\beta = 180°$; curves 1 to 4: $\eta = 0.001\,\text{N s/m}^2$; curve 5: $\eta = 0.0005\,\text{N s/m}^2$.

Under certain conditions, a paramagnetic particle, after passing near equilibrium point moves back and passes the equilibrium point

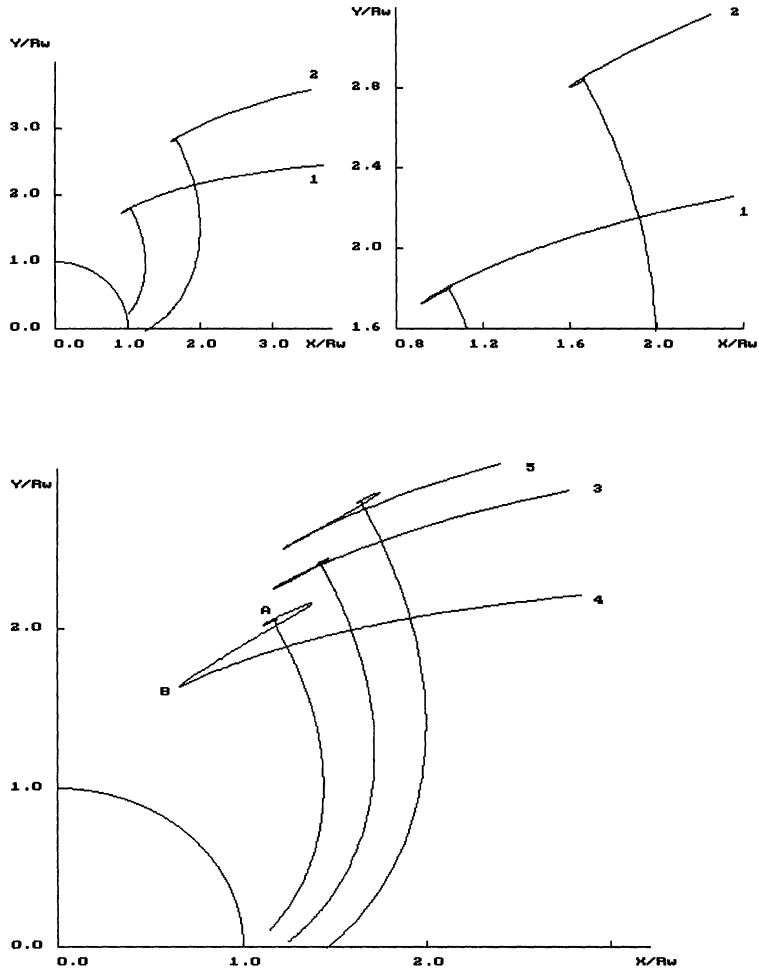

FIGURE 1 The limiting trajectories of ilmenite particles (curves 1 and 2) and wolframite particles (3, 4 and 5) in the vicinity of a cylindrical ferromagnetic element.

again. Sometimes it may do two or more cycles of oscillation motion near the equilibrium point and after that it moves away from this point (for example, a ferromagnetic element captures the particle or the flow removes it). Such a kind of trajectories of particle motion is shown in the Fig. 1 (curves 4, 5).

To find the amplitude of particle oscillation on a trajectory close to the limiting one we need to calculate the coordinates of the equilibrium point A and a turning point B (Fig. 1), at which the direction of the particle motion changes sharply. Let us consider the shortest distance between points A and B as the amplitude of particle oscillation. The angle of the direction of particle motion changing at point B may be close to 180°. The trajectory then has the form of a loop near the equilibrium point. This angle may be close to the right angle, then the trajectory has a sharp kink, point A merges with point B, and the oscillation amplitude is equal to zero.

Figure 2 shows the results of calculations of the normalized amplitude l/d_p (l is the amplitude, d_p is the particle diameter) depending on the magnetic induction B_0: lines 1–5 are for ilmenite particles, and line 6 is for wolframite particles. Other parameters are the following: $d_p = 100\,\mu m$ (lines 1–3) and $200\,\mu m$ (lines 4–6), cylinder diameter $d_w = 0.5\,mm$ (lines 1, 2) and $1\,mm$ (lines 3–6), flow velocity $\upsilon_0 =$ 0, 1 m/s (lines 1, 4, 6) and 0.2 m/s (lines 2, 3, 5). The gravitational force was neglected in these variants.

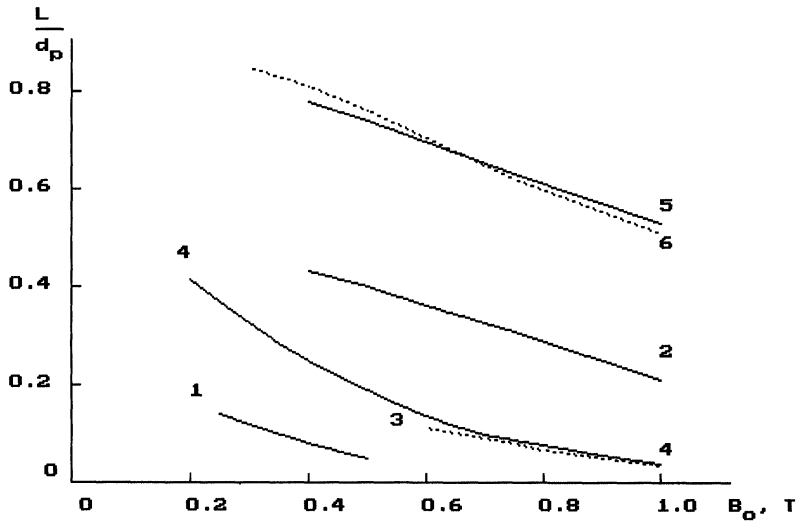

FIGURE 2 The relative amplitude of particle oscillation near the equilibrium point depending on magnetic induction.

It can be seen that in all the variants 1–6 the oscillation amplitude decreases with the increase of magnetic induction B_0. This can be explained by increasing the distance between the cylinder and the equilibrium point, which leads to the decrease of the magnetic and the hydrodynamic forces near the equilibrium point and to the decrease of the difference between these forces.

On the other hand, the decrease of the induction B_0 in all examples shown here and later was limited by a condition that the equilibrium point does not have to be too close to the cylinder surface. In the opposite case we would have to take into account the influence of the particle on flow velocity field around the cylinder and also the changing of the value *HgradH* within the particle volume. Comparing curves 1 and 2 (for particles with diameter $d_p = 100\,\mu\text{m}$, cylinder element diameter $d_w = 0.5\,\text{mm}$), and also curves 4 and 5 ($d_p = 200\,\mu\text{m}$ and $d_w = 1\,\text{mm}$) in Fig. 2, we can see that the oscillation amplitude increases with the increase of velocity $_0$. Comparison of curves 3 and 5 shows the increase of the oscillation amplitude depending on particle diameter d_p.

The increase of the oscillation amplitude, when any one of parameters d_p and $_0$ is increasing, can be explained by increase of the particle kinetic energy. The amplitude of particle oscillation increases depending on the decrease of the diameter of cylindrical ferromagnetic element, this can be seen by comparing curves 2 and 3 ($d_w = 0.5\,\text{mm}$ and 1 mm respectively). The increase of the magnetic and hydrodynamic forces gradients depending on the decrease of diameter d_w, when ratio r/r_w is constant (r is distance from cylinder axis to a point of the trajectory), can explain it.

The value of the oscillation amplitude of wolframite particles (curve 6) is greater than the value for ilmenite particles (curve 4), when values $d_p = 100\,\mu\text{m}$, $d_w = 1\,\text{mm}$, $\upsilon_0 = 0.1\,\text{m/s}$ are fixed. It can be explained by a higher density of wolframite and consequently (under the condition $d_p = \text{const}$) by a higher value of the kinetic energy of a wolframite particle. Since the conditions for calculation of curves 4 and 6 differ not only in particle density, but also in magnetic susceptibility, the effects of each factor are analyzed separately.

In Fig. 3 one can see the dependence of the oscillation amplitude on specific magnetic susceptibility χ_p, when the particle diameter $d_p = 200\,\mu\text{m}$ and density $\rho_p = 4.7 \times 10^3\,\text{kg/m}^3$, diameter of a cylindrical ferromagnetic element $d_w = 1\,\text{mm}$; $\upsilon_0 = 0.1\,\text{m/s}$, $B_0 = 0.3$, 0.5 and

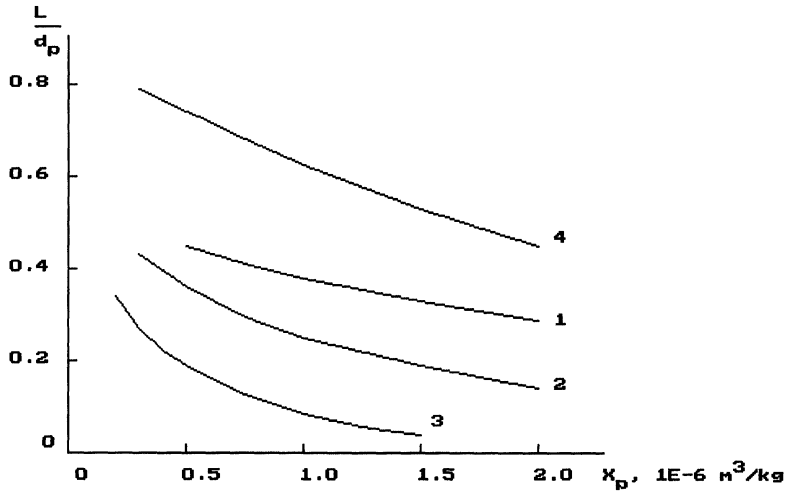

FIGURE 3 The relative amplitude of particle oscillation depending on specific magnetic susceptibility of a particle.

1 T for curves 1, 2 and 3 respectively; for curve 4 $B_0 = 1$ T, $v_0 = 0.2$ m/s. The gravitational force was neglected for calculation of these variants.

In all these cases the oscillation amplitude decreases, when the particle magnetic susceptibility increases. It is caused by the increase in the distance between the cylinder and the equilibrium point, and the corresponding decrease of the gradients of the magnetic and the hydrodynamic forces near the equilibrium point.

The character of the effect of the value χ_p on the oscillation amplitude is similar to the effect of value B_0: when χ_p or B_0 increases, parameter v_m also increases. It means that when $v_0 = \text{const}$, the normalized distance r_*/r_w increases too.

The difference is that the increase of χ_p and $B_0 = \text{const}$ does not lead to the change of the boundary between the dia- and paramagnetic capture zones. When B_0 increases and $\chi_p = \text{const}$, the zone of paramagnetic capture is reduced, line $F_{m,r} = 0$, which serves as a boundary between these two zones, moves to the line $y = x$. Calculations show that the polar angle of equilibrium point does not change much ($\theta_* \approx 60°$), when B_0 changes, that is why the above mentioned change of line $F_{m,r} = 0$, depending on the increase of B_0, means growth of

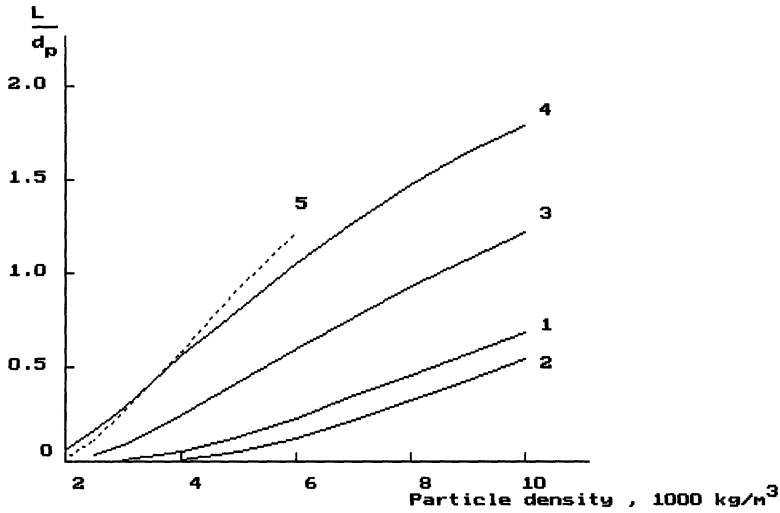

FIGURE 4 The relative amplitude of particle oscillation depending on particle density when the volumetric magnetic susceptibility is constant.

the relative length of a part of paramagnetic particle trajectory located in the diamagnetic capture zone.

Figure 4 shows the dependence of the normalized amplitude l/d_p of particle oscillation on its density ρ_p, under the following constant values: particle diameter $d_p = 200\,\mu m$, cylindrical ferromagnetic element diameter $d_w = 1\,mm$, and volumetric magnetic susceptibility $\kappa_p = 7.05 \times 10^{-3}$ (SI). Curves 1–4 were calculated ignoring the gravitational force F_g, while curve 5 includes the effect of F_g, when $\beta = \pi$ (vertically descending flow). For curves 1 and 2 – $B_0 = 0.15$ and $0.25\,T$ at $v_0 = 0.05\,m/s$; curves 3–5 – $B_0 = 0.25\,T$ at $v_0 = 0.1\,m/s$; curve 4 – $B_0 = 0.5\,T$ at $v_0 = 0.2\,m/s$.

In all cases the increase of the particle density ρ_p leads to the increase of the amplitude l/d_p of relative oscillation and the dependence $l/d_p(\rho_p)$ is close to linear, with the exception of curves whose initial parts correspond to small values of l/d_p.

Comparison of curves 3 and 5 in the Fig. 4 shows that by taking into account the gravitational force, when $\beta = \pi$, the amplitude of particle oscillation increases. It can be explained by increasing the velocity of particle motion relative to the cylinder under the influence of the

gravitational force in the descending flow. A similar increase of the particle velocity occurs when the flow velocity v_0 increases; it leads also to the increase of the oscillation amplitude: curve 3 for $v_0 = 0.1$ m/s is substantially higher than curve 2 for $v_0 = 0.05$ m/s.

If the vector of the gravitational force is opposite to vector $\vec{v}_0$ (vertical ascending flow), then the velocity of particle motion relative to the cylinder decreases, and correspondingly the amplitude of the particle oscillation decreases too. Trajectories of ilmenite particles for $d_p = 200$ μm, $d_w = 1$ mm, $B_0 = 0.3$ T, $v_0 = 0.1$ m/s are shown in Figs. 5a and 5b ; 5a shows the longitudinal effect of the gravitational force $\vec{F}_g$: 1 – $\beta = 0$ (vertical ascending flow), 2 – $\beta = \pi$ (descending flow), 3 – without taking gravitational force into account; 5b shows the transversal effect of $\vec{F}_g$: 1 – $\beta = -\pi/2$; 2 – $\beta = \pi/2$; 3 – without taking gravitational force into account.

As you can see in Fig. 5a, the amplitude of particle oscillation is much larger when $F_g \neq 0$ and $\beta = \pi$ than when $F_g = 0$, and much smaller when $F_g \neq 0$ and $\beta = 0$. Fig. 5b shows that when the gravitational force $\vec{F}_g$ influence is transversal, the oscillation amplitude does not change much, although the angle of the trajectory inclined changes substantially.

The increase of velocity v_0 leads to the decrease of the effect of the gravitational force on the oscillation amplitude. Figs. 6a and 6b shows the results of calculations of trajectory of an ilmenite particle when the values of parameters are equal to those used for examples shown in Figs. 5a and 5b, except for $B_0 = 0.5$ T, $v_0 = 0.2$ m/s used instead of $B_0 = 0.3$ T, $v_0 = 0.1$ m/s. The normalized distance r_*/r_w to the equilibration point when $F_g = 0$, is almost equal to the distance in preceding examples ($r_*/r_w \approx 2.4$ when B_0 3.0 T; $v_0 = 0.1$ m/s and $r_*/r_w \approx 2.3$ when $B_0 = 0.5$ T; $v_0 = 0.2$ m/s). Numbers of curves 1, 2 and 3 in Figs. 6a, 6b correspond to the conditions equal to the conditions used in Figs. 5a, 5b.

As you can see in Fig. 6a, the change of the oscillation amplitude under the condition of longitudinal influence of the gravitational force (when $\beta = 0$ and $\beta = \pi$ compared to the amplitude when $F_g = 0$) is less material than the same change shown in Fig. 5a. When the influence of the gravitational force is transversal and $v_0 = 0.2$ m/s (Fig. 6b), the oscillation amplitude almost does not change for three analogous cases: $F_g = 0$; $F_g \neq 0$ and $\beta = 0$; $F_g \neq 0$ and $\beta = \pi$.

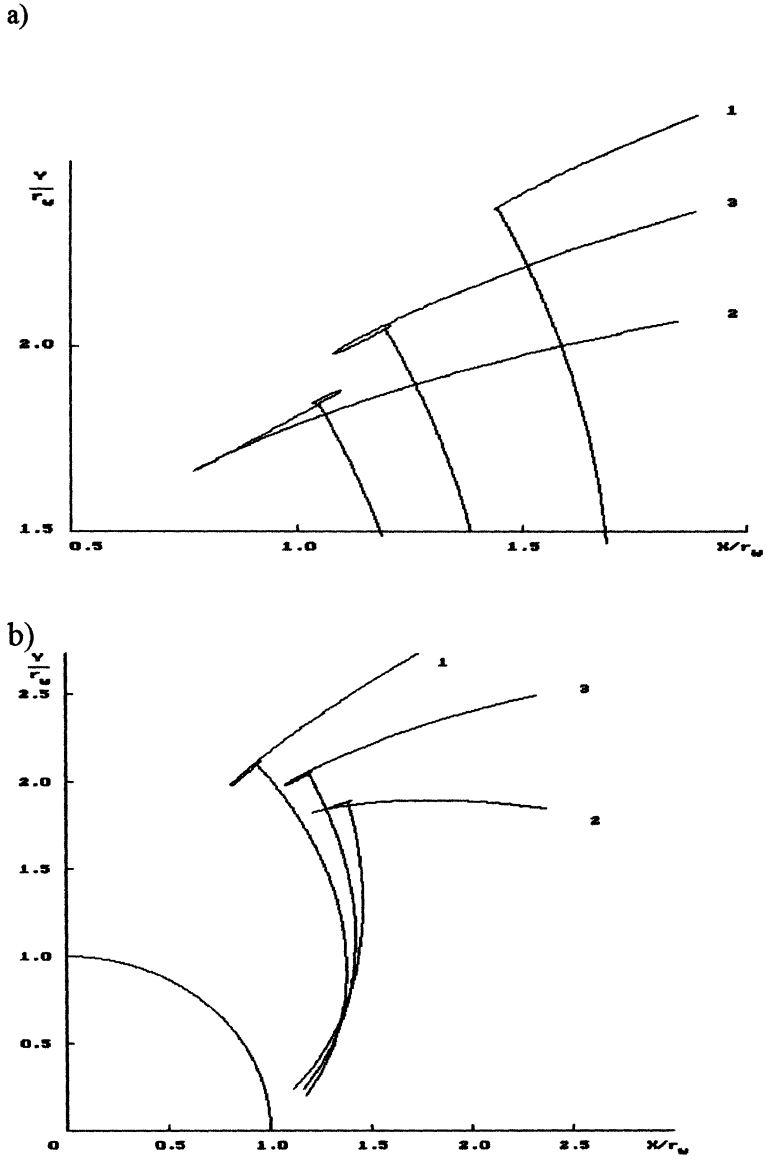

FIGURE 5 The limiting trajectories of ilmenite particles in the vicinity of cylindrical ferromagnetic elements under the condition of longitudinal (a) and the transversal (b) action of the gravitational force, $\upsilon_0 = 0.1$ m/s.

a)

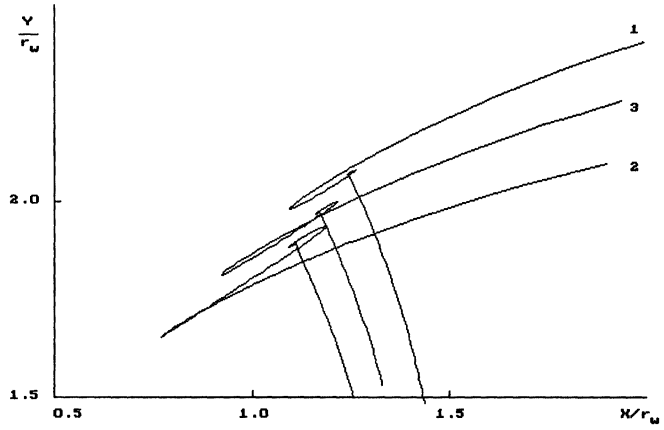

b)

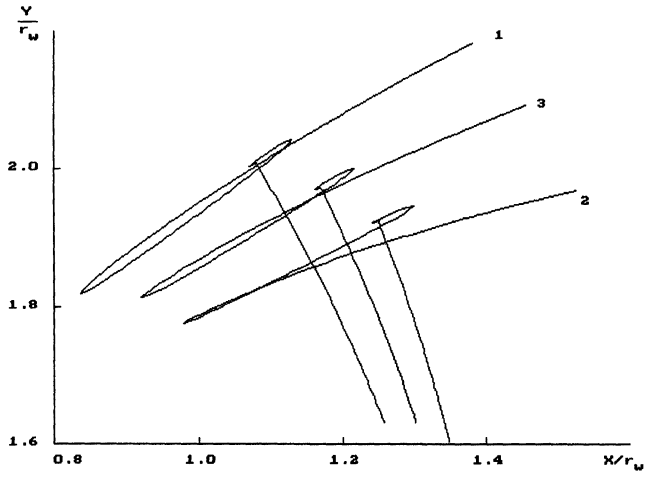

FIGURE 6 The limiting trajectories of ilmenite particles in the vicinity of cylindrical ferromagnetic elements under the condition of longitudinal (a) and the transversal (b) action of the gravitational force, $v_0 = 0.2\,\text{m/s}$.

3.2 The Time of a Particle Motion Along Trajectories Close to the Limiting Trajectory

When a particle moves to the equilibrium point, its velocity decreases, that is why the time of motion from the initial point of the trajectory (x_0, y_0) to the cylinder surface increases, compared to the time of the uniform motion at velocity υ_0. To get comparable date of the time of particle motion, we normalize the distance x_0 from the cylinder axis to the initial point: $x_0 = 3r_*$, where r_* is the distance to the equilibrium point. Further, we consider the ratio of the motion time τ to τ_0 (the time of the uniform motion at velocity υ_0): $\tau_0 = (x_0 - r_w)/\upsilon_0$, instead of the absolute value of the time of the motion.

Figure 7 shows the results of calculations of relative time of particle motion τ/τ_0 depending on the trajectory displacement compared to the limiting trajectory. The displacement can be defined as the ratio $(y_c - y_0)/y_c$ where y_c, y_0 are the ordinates of the limiting and any other trajectory when $x = x_0$.

Lines 1–4 show the results for $d_p = 100\,\mu\text{m}$; lines 5–8 for $d_p = 200\,\mu\text{m}$. For lines 1 and 3 – $d_w = 0.5\,\text{mm}$; in other cases $d_w = 1\,\text{mm}$. In examples 1, 2, 5, 6 – $\upsilon_0 = 0.1\,\text{m/s}$; in examples 3, 4, 7, 8 – $\upsilon_0 = 0.2\,\text{m/s}$; for curve 5 – $B_0 = 0.25\,\text{T}$, for curves 1, 2, 3, 4, 6, 7 – $B_0 = 0.5\,\text{T}$, for curve 8 – $B_0 = 1\,\text{T}$. In all examples $\rho_p = 4.7 \times 10^3 \text{kg/m}^3$; $\chi_p = 1.5 \times 10^{-6} \text{m}^3/\text{kg}$.

As can be seen in Fig. 7, the relative time τ/τ_0 depends linearly on logarithm of the value $(y_c - y_0)/y_c$. The results of calculations show that substantial deceleration of particles (increase of the motion time) is observed only in trajectories close to the limiting trajectory when $(y_c - y_0)/y_c = 0.001 - 0.01$ or less.

3.3 The Increase of Concentration of Magnetic Particles Near the Equilibrium Point

Let us suppose that the initial section $x = x_0$ is far enough from a cylindrical collector to ensure that the distribution of magnetic particles is uniform. It means that on any fixed trajectory the particles pass through a section $x = \text{const}$ in equal time intervals $\Delta\tau$. While a particle moves along the trajectory, the distance Δl_i between two nearest (with numbers i and $i+1$) particles on the trajectory changes according to formula $\Delta l_i = \int_{\tau_i}^{\tau_i + \Delta\tau} \upsilon_p(\tau) d\tau$, were υ_p is the particle

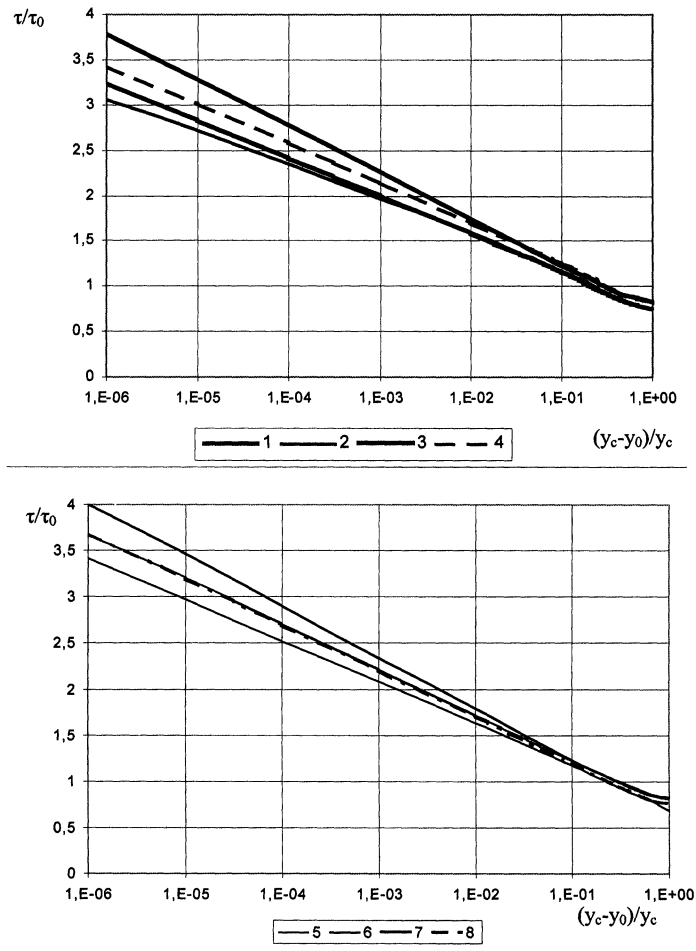

FIGURE 7 The relative time of particle motion depending on trajectory displacement compared to the limiting trajectory.

velocity at the current point of the trajectory. Near the equilibrium point the particle velocity v_p is small, and the distance Δl between two nearest particles on the trajectory is small too. The results of calculations of a position of ilmenite particles with diameter 100 μm along four trajectories are shown in Fig. 8; when at the initial section $x = x_0$ the ordinates of the trajectories are equal to $\tilde{y}_0 = 2.0$, 2.4, 2.6, 3.0; $v_0 = 0.2$ m/s; $d_w = 1$ mm; $B_0 = 0.75$ T.

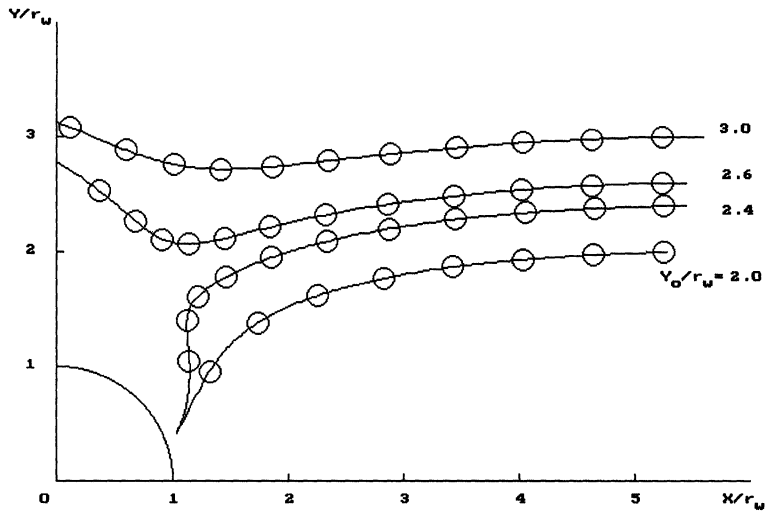

FIGURE 8 The change of the mutual location of particles along trajectories in a region close to the equilibrium point.

Two middle trajectories pass near the equilibrium point and have in that area much greater curvature than in other parts. The distance Δl_i between particles on one trajectory near the equilibrium point is much less than on the initial part of the trajectory. This change of mutual location of particles can lead to an increase of their concentration near the equilibrium point. However, these results do not allow us to consider this conclusion as enough well-proven. A stricter analysis which would take into account the longitudinal distance between particles as well as perpendicular to the trajectory is required.

4. CONCLUSIONS

As a result of numerical calculations of equations of motion of a paramagnetic particle in a working zone of a separator with cylindrical ferromagnetic elements, the configurations of particle trajectories near the equilibrium point were investigated. It was shown that under conditions of certain combinations of technological parameters and particle characteristics the particle motion near the equilibrium point has a character of oscillation. The oscillation amplitude

increases with the decrease of the distance from a cylindrical element to the equilibrium point. When the distance is fixed, the oscillation amplitude increases with the increase of particle size and density, carrying fluid velocity and with the decrease of its viscosity. In our analysis only those combinations of parameters when the equilibrium point and the nearest to the cylinder point of return are at a distance of several particles diameters or more from the cylinder were considered. Further limitation is that we did not take into account the particle influence on flow velocities near the cylinder. Furthermore, the amplitude of particle oscillation increases with the decrease of the cylindrical element diameter d_w (value of diameter d_w is limited by relation $d_w/d_p = 4$–5 and more).

It was shown that the time τ of motion from the initial point to the cylinder surface increases depending on proximity of particle trajectory to the limiting trajectory. The dependence of τ on parameter $lg((y_c - y_0)/y_c)$ is almost linear.

NOMENCLATURE

B magnetic induction (Tesla);
H magnetic field strength (A/m);
M magnetization (A/m);
κ volume magnetic susceptibility (dimensionless unit of SI system);
χ specific magnetic susceptibility (m^3/kg);
μ magnetic permeability (H/m);
μ_0 $4\,\pi\,10^{-7}$ H/m;
t and τ time (s);
g acceleration of gravity (m/s^2);
v velocity (m/s);
d diameter (m or μm);
r radius (m);
$\tilde{r}$ dimensionless radius;
θ angle;
ρ density (kg/m^3);
η dynamic viscosity of the fluid (kg/m s);
C_d hydrodynamic drag coefficient (dimensionless);
F force (N).

References

[1] J. Svoboda (1987). *Magnetic Methods for the Treatment of Minerals*, p. 692. Elsevier, Amsterdam.
[2] E. Madai (1980). Teilcheneinfang Durch Magnetisierte Drahte bei der Hochgradientenmagnetscheidung. *Neue Bergbautechnik*, **10**(7).
[3] Yu. S. Mostyka, V.I. Karmazin, V. Yu. Shutov and L.Z. Grebenyuk (1999). *Magn. Electr. Sep.*, **10**, 35.

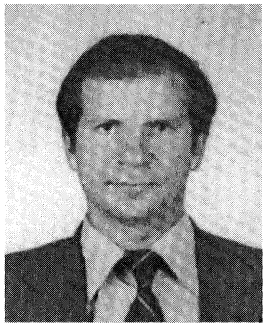

Youry Mostyka graduated from the Dnepropetrovsky Mining Institute in 1977 and acquired profession of mining engineer-electrician. In 1986, he obtained Ph.D. degree (Candidate of Technical Science) in mineral processing. His main area of interest is magnetic properties of minerals, theoretical and experimental research into separation of weakly magnetic ores and beneficiation of ores in strong magnetic fields and kinetics of high-gradient magnetic separation. Practical work is concerned with design of technology and equipment for beneficiation of ilmenite, rutile, zirconium ores, feldspar and garnet.

Valery Shutov graduated from the Electrotechnical Department of the Dnepropetrovsky Mining Institute in 1982. He started his career as an engineer at sub-faculty of industrial Process Automation. Since 1991, he works as a research officer at the National Mining Academy of Ukraine, Dnepropetrovsk. His field of scientific interest is the development of technological processes for coal and quartz sand beneficiation, research and design of experimental superconducting separators and automatic control systems.